

REPORT DO

AD-A238 791

Form Approved
OMB No. 0704-01881a. REPORT SECURITY CLASSIFICATION
Unclassified

2a. SECURITY CLASSIFICATION AUTHORITY

2b. DECLASSIFICATION/DOWNGRADING SCHEDULE

4. PERFORMING ORGANIZATION REPORT NUMBER(S)

3. DISTRIBUTION/AVAILABILITY OF REPORT
Approved for public release;
Distribution unlimited.

5. MONITORING ORGANIZATION REPORT NUMBER(S)

AFOSR-TR- 91 0037

6a. NAME OF PERFORMING ORGANIZATION
University of Calif., San Diego6b. OFFICE SYMBOL
(if applicable)7a. NAME OF MONITORING ORGANIZATION
AFOSR/NC

6c. ADDRESS (City, State, and ZIP Code)

Department of Chemistry, 0506
La Jolla, CA 92093-0506

7b. ADDRESS (City, State, and ZIP Code)

Bldg. 410
Bolling AFB, D.C. 20332-64488a. NAME OF FUNDING/SPONSORING
ORGANIZATION AFOSR8b. OFFICE SYMBOL
(if applicable)
NC9. PROCUREMENT INSTRUMENT IDENTIFICATION NUMBER
AFOSR-89-0174

8c. ADDRESS (City, State, and ZIP Code)

Bldg. 410
Bolling AFB, D.C. 20332-6448

10. SOURCE OF FUNDING NUMBERS

PROGRAM
ELEMENT NO.
61102FPROJECT
NO.
3484TASK
NO.
A2WORK UNIT
ACCESSION NO.

11. TITLE (Include Security Classification)

(U) DURIP Synthesis and Study of Preceramic Polymers/Ceramic Precursors, Metal Silicides, and Polymer with Unique Optical and Electronic Properties

12. PERSONAL AUTHOR(S)

T. Don Tilley

13a. TYPE OF REPORT
Final Technical13b. TIME COVERED
FROM 12/1/89 TO 11/30/9014. DATE OF REPORT (Year, Month, Day)
5/23/9115. PAGE COUNT
15

16. SUPPLEMENTARY NOTATION

17. COSATI CODES

FIELD GROUP SUB-GROUP

18. SUBJECT TERMS (Continue on reverse if necessary and identify by block number)

19. ABSTRACT (Continue on reverse if necessary and identify by block number)

The thermal analysis system and tube furnace purchased on this grant have been used to conduct initial studies on the conversion of alkoxysiloxy derivatives to metal silicate solid state materials. These results, pertaining to titanium, zirconium, and hafnium, are described.

91-05935

91 7 23 014

20. DISTRIBUTION/AVAILABILITY OF ABSTRACT

☐ UNCLASSIFIED/UNLIMITED ☒ SAME AS RPT. ☐ DTIC USERS

21. ABSTRACT SECURITY CLASSIFICATION

Unclassified

22a. NAME OF RESPONSIBLE INDIVIDUAL

Dr. Fred Hedberg

22b. TELEPHONE (Include Area Code)

202-767-4960

22c. OFFICE SYMBOL

NC

DURIP Synthesis and Study of Preceramic Polymers/Ceramic Precursors, Metal Silicides, and Polymers with Unique Optical and Electronic Properties

Final Technical Report

The thermal analysis system and tube furnace purchased on this grant have been used to conduct initial studies on the conversion of alkoxysiloxy derivatives to metal silicate solid state materials. These results, pertaining to titanium, zirconium, and hafnium, are described below.

Interest in low-temperature chemical routes to ceramic materials is based largely on the potential for generating metastable structures with unusual properties, or on development of improved processing methods. The sol-gel method in particular has attracted attention as a low-temperature route to oxide materials.¹ This method can be extended to the synthesis of mixed-metal oxides, however the formation of homogeneous materials can be complicated by differences in hydrolysis rates for the starting metal compounds.² Nonetheless, sol-gel processes have been utilized to produce (for example) TiO_2 - or ZrO_2 -containing silicates in the form of thin films, fibers, or monoliths.³ Materials of this type find applications that take advantage of their optical properties, chemical inertness, high melting points, insulating properties, and fracture toughness.

We are investigating use of (alkoxy)siloxy transition metal complexes as single source precursors to homogeneous metal silicate networks, and here report preliminary results regarding low-temperature conversion of the compounds $\text{M}[\text{OSi}(\text{O}^i\text{Bu})_3]_4$ [$\text{M} = \text{Ti}$ (1), Zr (2), Hf (3)] to $\text{MO}_2\cdot 4\text{SiO}_2$ materials. As siloxide precursors to silicates, these compounds have the advantage that the transition metal and silicon atoms are initially bonded only to oxygen. Also, the *tert*-butoxy groups undergo thermal elimination of isobutylene, which cleanly remove all the carbon as volatile material. Given the chemistry involved in the resulting condensation steps, silicate

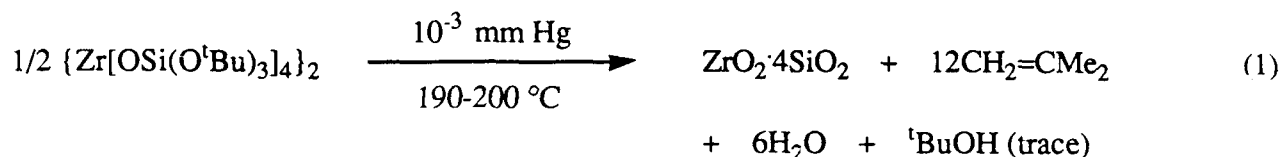
Best Available Copy

networks containing a homogeneous distribution of transition metal ions are expected to form. Here we show that these reactions can be employed to cast thin films, and to generate rather unusual microstructures. Hrnair has previously shown that zirconium and hafnium siloxides of the type $M(OSiR_3)_4$ ($R_3 = Et_3, Me_2^iBu, Me_2Ph, MePh_2, Ph_3$) decompose over a wide temperature range (350-600°C) to give $MO_2 \cdot 4SiO_2$ materials.⁴

Crystalline, pentane-soluble 1-3 were prepared by reactions of the appropriate amido derivatives, $M(NEt_2)_4$, with 4 equivalents of $HOSi(O^iBu)_3$ in pentane. In benzene solution, 1 and 3 are monomeric whereas 2 exists as a dimer. Abe has previously reported a synthesis for 2, and has described titanium derivatives related to 1. Compounds 1-3 undergo hydrolysis to liberate $HOSi(O^iBu)_3$ and produce metal oxide gels.

Thermal gravimetric analysis (TGA) curves for 1-3 (Figure 1) show precipitous weight losses corresponding to elimination of isobutylene and water.⁷ Minimal dehydration continues slowly thereafter, until a constant weight corresponding to quantitative formation of $MO_2 \cdot 4SiO_2$ is established. These thermolyses occur at remarkably low temperatures, particularly for 2 and 3 which exhibit onset temperatures of 137 and 141°C, respectively. The higher temperature required for decomposition of 1 may result from greater steric crowding about the smaller titanium center, which could restrict the molecular motion required for decomposition. The volatile products of thermolysis of 2 at 190-200°C (5 min) were collected by vacuum transfer, and identified as isobutylene (11.7 equivalents/Zr), water (5.4 equivalents/Zr), and *tert*-butanol (trace). This stoichiometry is approximately represented by equation 1.

| | |
|--------------------|--|
| Prepared For | |
| Project | |
| Prepared By | |
| Reviewed By | |
| Justification | |
| by | |
| Distribution/ | |
| Availability Codes | |
| Avail and/or | |
| Special | |
| Dist | |
| A-1 | |



Crystallizations and phase transformations were followed by X-ray powder diffraction (XRD), differential thermal analysis (DTA), and electron microscopy. The $\text{ZrO}_2 \cdot 4\text{SiO}_2$ system has been examined in greatest detail. Surprisingly, crystals of **2** retain their shape and morphology (in going from transparent to opaque) after decomposition at $1200\text{ }^\circ\text{C}$, with very little shrinkage ($\leq 10\%$). Samples of $\text{ZrO}_2 \cdot 4\text{SiO}_2$ are amorphous to $1100\text{ }^\circ\text{C}$ (by XRD), and an exothermic process at $1150\text{--}1400\text{ }^\circ\text{C}$ (observed by DTA) corresponds to crystallization of finely dispersed *t*- ZrO_2 . Heating $\text{ZrO}_2 \cdot 4\text{SiO}_2$ to $1500\text{ }^\circ\text{C}$ for 6 h under argon produces a mixture of *m*- ZrO_2 , *t*- ZrO_2 (1:5 ratio), and cristobalite.⁸ Rapid quenching of $\text{ZrO}_2 \cdot 4\text{SiO}_2$ from $1500\text{ }^\circ\text{C}$ to $0\text{ }^\circ\text{C}$ gave a material for which the ratio of *m*- ZrO_2 to *t*- ZrO_2 was maintained.

Transmission electron micrographs (TEM's) of samples of **2** decomposed at $400\text{ }^\circ\text{C}$ (2 h in an O_2 flow) reveal a fibrous structure (Figure 2a), which is characterized by a surface area of $118\text{ m}^2\text{ g}^{-1}$ (BET method). Further heating to $800\text{ }^\circ\text{C}$ (4 h, O_2) produces an ordered, interpenetrating network of thin fibers (Figure 2b), and a surface area of $82\text{ m}^2\text{ g}^{-1}$. The crystallization of zirconia at $1200\text{ }^\circ\text{C}$ (4 h, O_2) is apparent in TEM photographs (Figure 2c), which show small crystallites (6–21 nm) embedded in an amorphous silica matrix. The sintering that results from the latter thermal treatment reduces the surface area to $36\text{ m}^2\text{ g}^{-1}$.

Whereas the thermolysis chemistry of **3** and **4** appears to be quite similar, there are significant differences in the materials that are generated. The $\text{HfO}_2 \cdot 4\text{SiO}_2$ material produced at $400\text{ }^\circ\text{C}$ (2 h, O_2) is composed of 8–32 nm particles (Figure 2d). In samples heated to $1000\text{ }^\circ\text{C}$, *t*- HfO_2 (or *c*- HfO_2) is present, and samples taken to $1460\text{ }^\circ\text{C}$ contain *t*- HfO_2 (or *c*- HfO_2), *m*- HfO_2 (in roughly equal amounts), and cristobalite.

Heating **1** to 400 °C results in amorphous $\text{TiO}_2 \cdot 4\text{SiO}_2$, from which finely dispersed anatase crystallizes at 1000 °C (by XRD). Samples taken to 1400 °C contain anatase, rutile, and cristobalite.

The low temperatures at which **2** and **3** thermally decompose allow for formation of the silicate networks to be conveniently be carried out in solution. Refluxing **2** in xylenes for 10 h produces viscous, nearly transparent fluids and small amounts of particulate matter. Removal of the volatiles in vacuo leaves a white, amorphous $\text{ZrSi}_4\text{O}_x(\text{OH})_y$ powder that has a BET surface area of $520 \text{ m}^2 \text{ g}^{-1}$, and loses 27% of its weight when heated to 1150°C (by TGA). This powder is composed of ca. 0.1-3 μm agglomerates (by scanning electron microscopy) made from smaller, non-spherical 30-70 nm particles (by TEM). The dehydration of $\text{ZrSi}_4\text{O}_x(\text{OH})_y$ was monitored by ^{29}Si NMR spectroscopy of the isolated powder (dried in vacuo), which revealed a very broad peak which moved from -99 to -110 ppm as the sample was heated from 25 to 1200 °C. Annealing this material at 1200 °C (4 h, O_2) results in a significant reduction of the surface area to ca. $3 \text{ m}^2 \text{ g}^{-1}$. At higher temperatures, the same crystallization behavior described above for $\text{ZrO}_2 \cdot 4\text{SiO}_2$ is observed.

Hydrocarbon solutions of **2** and **3** have been used to cast thin films of $\text{ZrO}_2 \cdot 4\text{SiO}_2$ and $\text{HfO}_2 \cdot 4\text{SiO}_2$ onto quartz. For example, a 1% solution of **2** in benzene was spun onto a quartz disk, and the disk was then heated to 400 °C under O_2 for 30 min. Examination of the resulting film by SEM (Figure 3) revealed a smooth, crack-free surface. Similar $\text{HfO}_2 \cdot 4\text{SiO}_2$ films prepared from a 1% solution of **3** in cyclopentanone have thicknesses ranging from 70 to 90 nm (Dektak 3030 profilometer).

In conclusion, the chemical thermolyses described here represent an alternative approach to the synthesis of silicate materials. The solid state conversions produce porous ceramic materials that can have ordered microstructures. Continuing investigations are attempting to probe the

possibility that formation of such microstructures may be controlled via directionality imposed on the condensation process by the crystalline lattice of the precursor compound. The chemistry involved in this process can be applied to sol gel-like processes in non-polar media, and should allow the homogeneous incorporation of a wide variety of dopants (e.g., polymers or additional metal ions). We are currently investigating the use of the gel-like $[\text{MSi}_4\text{O}_x(\text{OH})_y]_z$ solutions for fashioning films, fibers and monoliths.

REFERENCES

- 1 See for example: *Sol-Gel Technology for Thin Films, Fibers, Preforms, Electronics, and Specialty Shapes*, edited by L. C. Klein (Noyes Publications, Park Ridge, New Jersey, 1988); D. R. Ulrich, in *Transformation of Organometallics into Common and Exotic Materials: Design and Activation*, NATO ASI Series E: Appl. Sci. No 141, edited by R. M. Laine (Martinus Nijhoff Publishers, Amsterdam, 1988), p. 103; H. Schmidt, *J. Non-Cryst. Solids* **100**, 51 (1988).
- 2 D. R. Uhlmann, B. J. J. Zelinski, and G. E. Wnek in *Better Ceramics Through Chemistry* (Materials Research Society Symposia Proceedings, Vol. 32), edited by C. J. Brinker, D. E. Clark, and D. R. Ulrich (North-Holland, New York, 1984), p. 59.
- 3 T. Gunji, Y. Nagao, T. Misono, and Y. Abe, *J. Non-Cryst. Solids* **107**, 149 (1989); I. M. M. Salvado, C. J. Serna, J. M. F. Navarro, *J. Non-Cryst. Solids* **100**, 330 (1988); M. Nogami and M. Tomozawa, *J. Am. Ceram. Soc.* **69**, 99 (1986); V. S. Nagarjan and K. J. Rao, *J. Mater. Sci.* **24**, 2140 (1989); K. Kamiya, S. Mabe, T. Yoko, and K. Tanaka, *J. Ceram. Soc. Jpn. Inter. Ed.* **97**, 227 (1989); M. Nogami, *J. Non-Cryst. Solids* **69**, 415 (1985); D. Kundu, P. K. Biswas, and D. Ganguli, *J. Non-Cryst. Solids* **110**, 13 (1989).
- 4 D. C. Hrnčir and G. D. Skiles, *J. Mater. Res.* **3**, 410 (1988).
- 5 Y. Abe, K. Hayama, and I. Kijima, *Bull. Chem. Soc. Japan* **45**, 1258 (1972).
- 6 Y. Abe and I. Kijima, *Bull. Chem. Soc. Japan* **43**, 466 (1970).
- 7 Thermal analyses were obtained with a Du Pont Model 2000 system.
- 8 $\text{MO}_2\cdot 4\text{SiO}_2$ samples were quenched in air to room temperature unless otherwise noted.

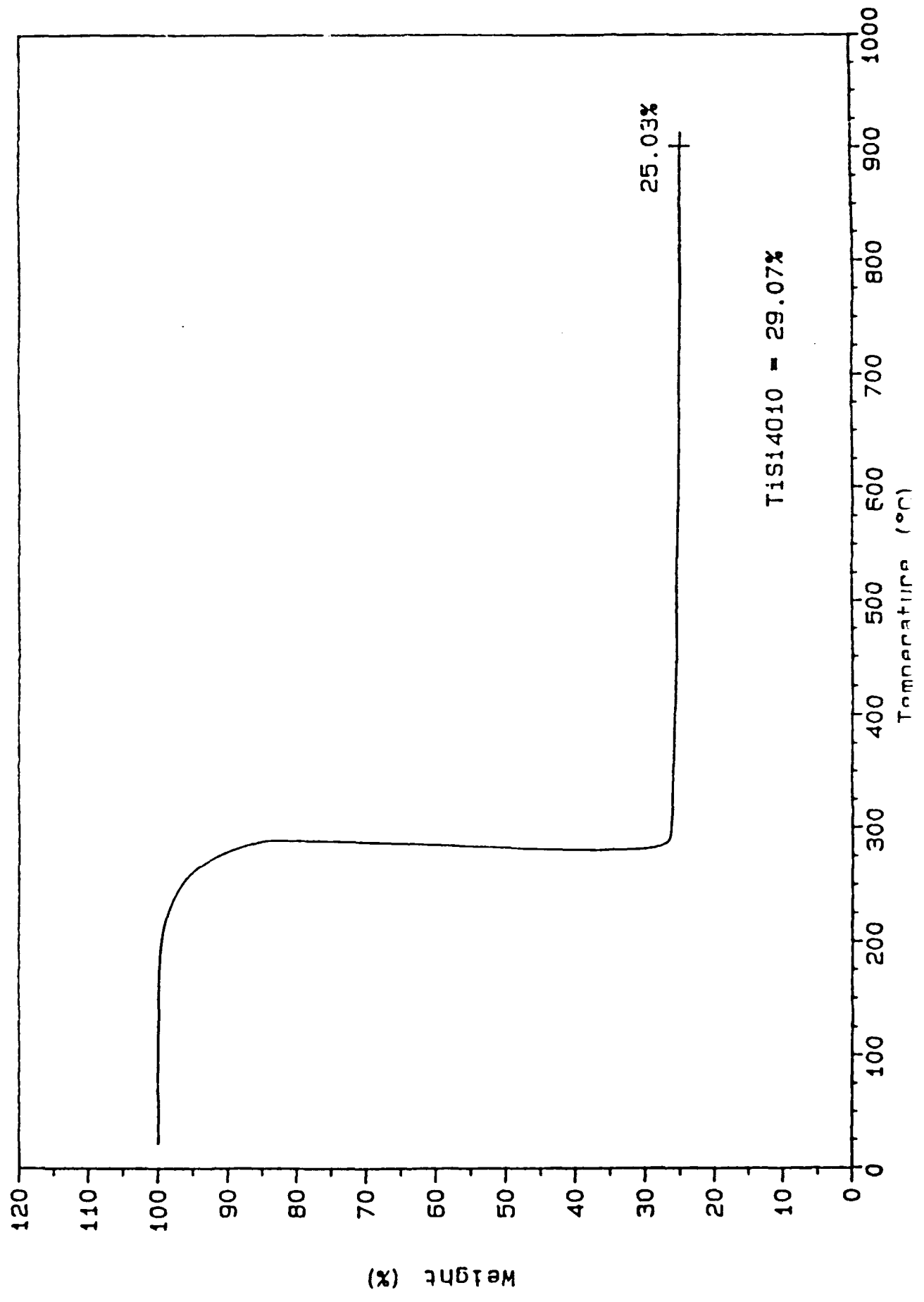
Figure Captions

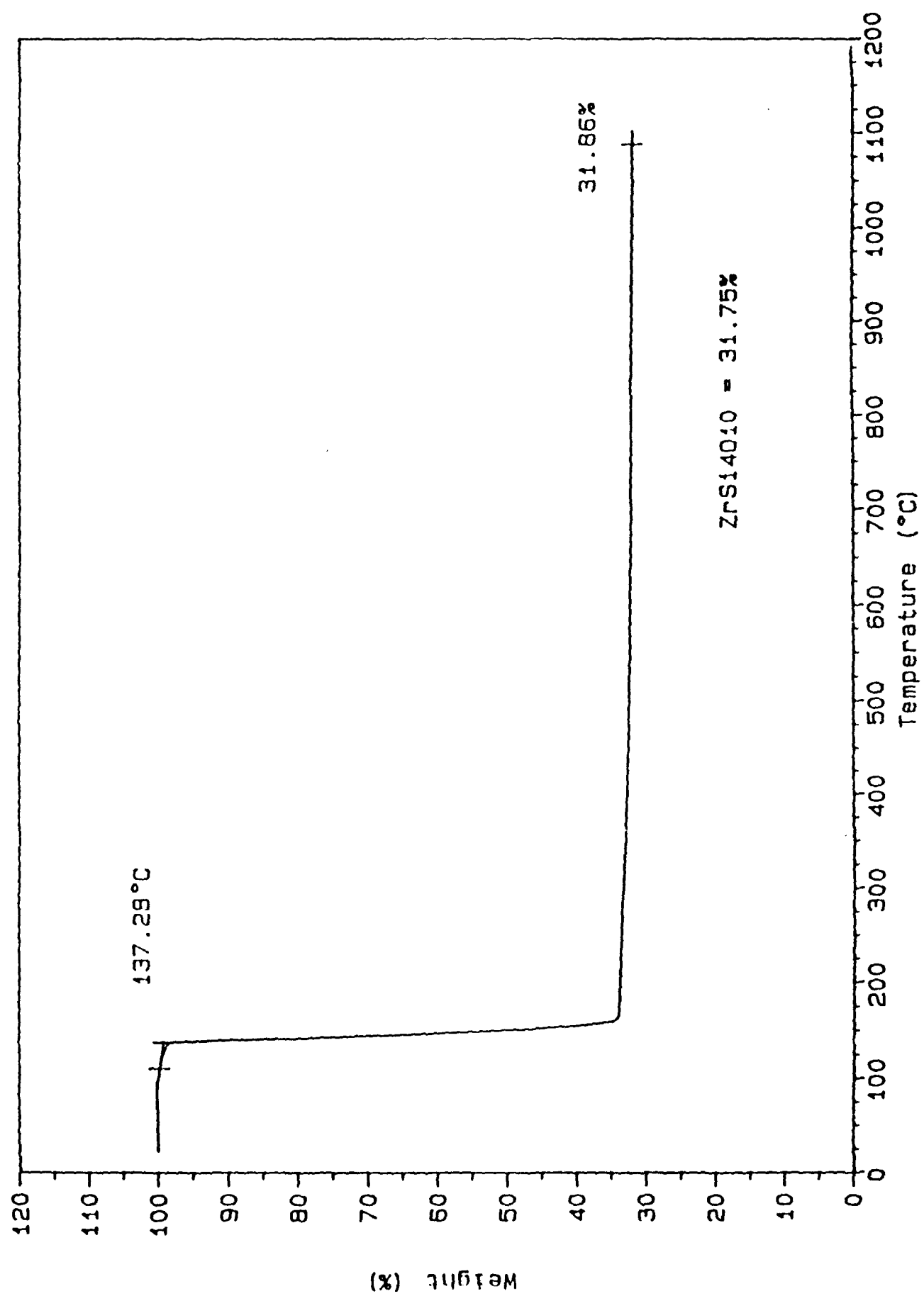
Figure 1. (a) TGA of **1** ($2\text{ }^{\circ}\text{C min}^{-1}$ to $450\text{ }^{\circ}\text{C}$; $20\text{ }^{\circ}\text{C min}^{-1}$ to $900\text{ }^{\circ}\text{C}$). (b) TGA of **2** ($2\text{ }^{\circ}\text{C min}^{-1}$ to $200\text{ }^{\circ}\text{C}$; $20\text{ }^{\circ}\text{C min}^{-1}$ to $1100\text{ }^{\circ}\text{C}$). (c) TGA of **3** ($2\text{ }^{\circ}\text{C min}^{-1}$ to $200\text{ }^{\circ}\text{C}$; $20\text{ }^{\circ}\text{C min}^{-1}$ to $1100\text{ }^{\circ}\text{C}$).

Figure 2. TEM micrographs of material from decomposed **2** and **3**. (a) $\text{ZrO}_2\cdot 4\text{SiO}_2$ heated to $400\text{ }^{\circ}\text{C}$ (2 h, O_2). (b) $\text{ZrO}_2\cdot 4\text{SiO}_2$ heated to $800\text{ }^{\circ}\text{C}$ (4 h, O_2). (c) $\text{ZrO}_2\cdot 4\text{SiO}_2$ heated to $1200\text{ }^{\circ}\text{C}$ (4 h, O_2). (d) $\text{HfO}_2\cdot 4\text{SiO}_2$ heated to $400\text{ }^{\circ}\text{C}$ (2 h, O_2).

Figure 3. SEM micrograph of $\text{ZrO}_2\cdot 4\text{SiO}_2$ thin film spun onto quartz from a 1% solution of **2** in benzene.

Figure 1a





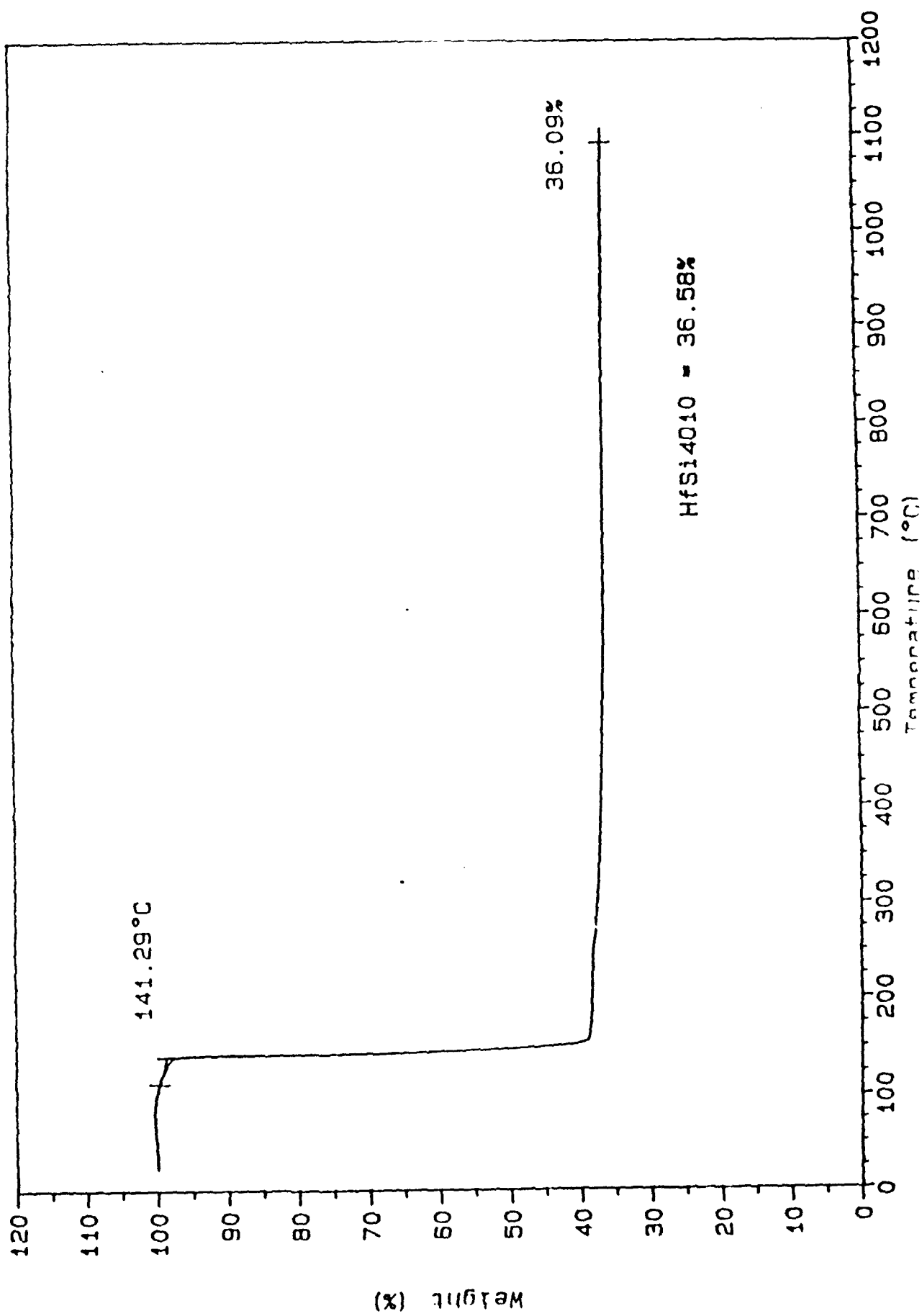
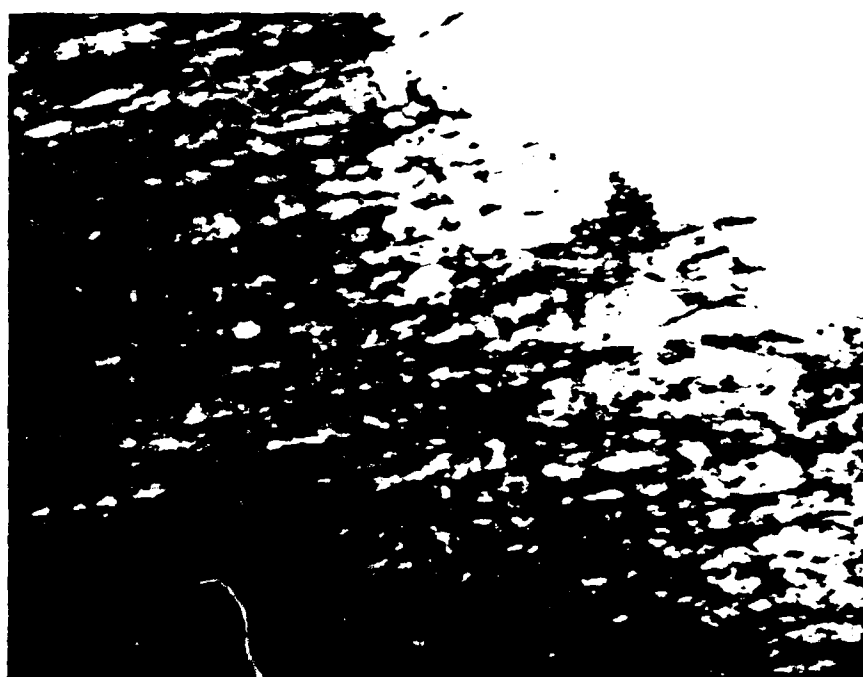


Figure 2a



250 nm

Figure 2b



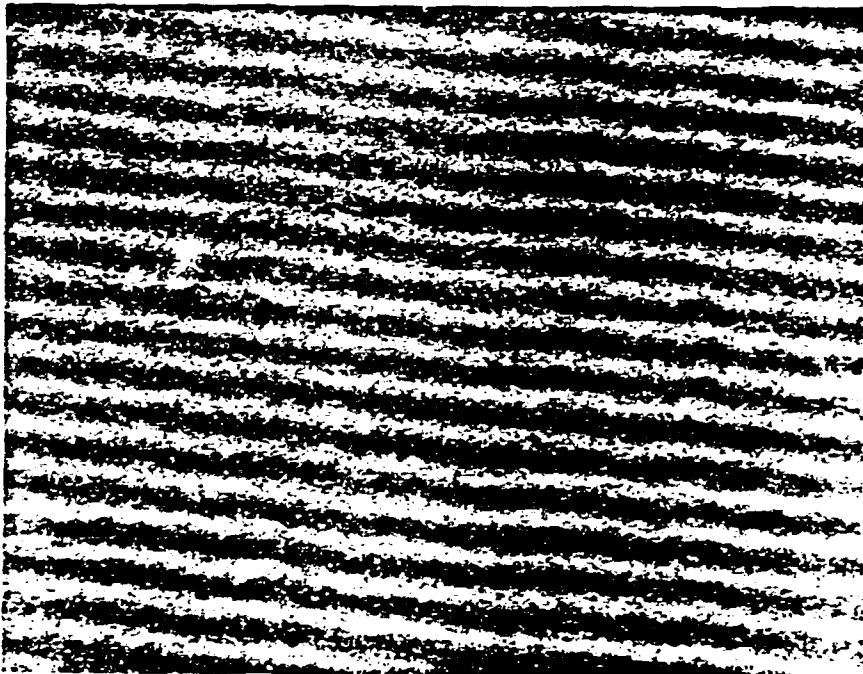
200 nm

Figure 2c



100 nm

Figure 3



300 nm